SUPPLEMENTARY DATA

SUPPLEMENTARY MATERIALS AND METHODS

Scanning electron microscopy

To prepare collagen solutions, Col I in 0.01 N HCl (PureCol [atelo-type I collagen], Advanced Biomatrix Cat# 5005) or telo-Col I (RatCol [telo-type I collagen], Advanced Biomatrix Cat# 5153) was neutralized (to pH 7.0±0.2) on ice by adding 0.1 M NaOH and mixed with 10X PBS to yield a stock solution containing 2 mg/mL (~6.67 µM) collagen in 1X PBS. Recombinant murine WISP1 (R and D systems Cat# 1680-WS) in PBS or recombinant human WISP2 (PeproTech Cat# 120-16) were added at a final concentration of 50 µg/mL and 100 µg/mL respectively, unless otherwise indicated. The pH of the final collagen + analyte solutions was measured with an Orion PerpHecT ROSS Combination pH Micro Electrode (Thermo Fisher Scientific) and was confirmed to be constant across conditions. 50 µL of collagen solution was transferred to a 16-well glass slide (Thermo Fisher Scientific) and incubated at 37ºC for 4h (Col I) or at room temperature for 2 h (telo-Col I) to allow for fibril formation. Collagen lattices were then fixed in 2.5% glutaraldehyde, 2% paraformaldehyde in 0.1 M $CaCO_4$ and processed for scanning electron microscopy at the St. Jude Children's Research Hospital Cell & Tissue Imaging Center as previously described (1). Briefly, samples were first rinsed in 0.10 M cacodylate buffer (4 × 5 min) followed by a secondary fixation in 1% OsO_4 in water for 60 min. They were then rinsed (4 × 5 min) in ultrapure water followed by dehydration in a graded ethanol series (30%, 50%, 70%, 90%, 100% ×2) for 10 min per step. The samples were then loaded into an Autosamdri 931.GL critical point dryer (Tousimis), which was set to perform 3 CO_2 exchanges. The samples were then mounted on aluminum stubs by using conductive carbon

adhesive tabs, sputter-coated with 28 nm of iridium (Desk V, Denton Vacuum), and imaged with a Field Emission Scanning Electron Microscope (FEI-Thermo Fisher) and MAPS software (FEI-Thermo Fisher).

Images were analyzed as described previously (1). For each image, the curvature ratio of the collagen fibrils was determined with NIH ImageJ (ImageJ, RRID:SCR_003070) by drawing segmented lines along the length of the fibrils (A) and a single straight line between the start and end of the fibrils (B). The curvature ratio of the collagen fibrils was then calculated by dividing the length of A by the length of B. The curvature ratio was determined for 5 fibrils per image in 5 images per lattice. The numbers of "hairpin- or end-like" structures (fibrils that end or that form sharp bends at angles of 45º or less) and of "knot-like" structures (areas of tangled fibrils) in each 72 μm^2 image were counted. To measure the diameter (width) of fibrils in Col I lattices, in focus fibrils in SEM images were segmented using the Autocontex machine-learning method implemented in the open-source ilastik software package (2, 3). The FibrilJ plugin in ImageJ was then used to quantify fibril width (4). Average fibril width was calculated from > 30 data points per image. The diameters of larger fibril bundles in telo-Col I images were measured in NIH ImageJ, and the measurements for the 5 largest bundles in each image were averaged (5 images/lattice).

Generation of stable cell lines

To generate 4T1 and MDA-MB-231 tumor cells with stable murine or human *WISP1* or *WISP2* overexpression, respectively, murine and human *WISP1* and *WISP2* cDNAs (gBlock, IDT) were cloned into the pCDH-EF1-MCS-T2A-puro lentiviral vector (System Biosciences) downstream

of the EF1 promoter by Mega primer RF cloning, following the IDT protocol. Using the same approach, a gBlock coding for the CT domain of *Wisp1* (Table S1) was inserted into the pCDH-EF1-Wisp2-T2A-puro vector to generate the pCDH-EF1-Wisp2+CT-T2A-puro vector. Cell lines with stable overexpression of *Wisp1* lacking its CT domain (*Wisp1ΔCT*) or Myc-tagged *Wisp1* were generated with the QuikChange Lightning Site-directed mutagenesis kit (Agilent Technologies) and the primers listed in Table S2. Packaging of the vector was obtained by co-transfecting 293FT cells with 2 μg transfer vector, 1 μg pCMV-dR8.9, and 1 μg VSVg expression vectors using TransIT-293 reagent (Mirus) in Opti-MEM I (Thermo Fisher). 48 h after transfection, 293FT cell–conditioned medium was collected, filtered through a 0.45-μm filter, and applied to tumor cells with 4 μg/mL polybrene (Sigma). The tumor cells were then selected with 5 μg/mL puromycin beginning 24 h after transduction.

For stable knockdown of *Wisp1*, 4T1 cells were initially transduced with the doxycyclin-inducible pCW-Cas9-Blast vector (gift from Mohan Babu; RRID: Addgene_83481) to establish a 4T1-indCas9 stable cell line by blasticidin selection. The 4T1-indCas9 stable cells were further transduced with a pool of 3 control non-targeting gRNAs or a pool of 5 Wisp1-targeting gRNAs (Table S3) lentiGuide-puro vectors (gift from Feng Zhang; RRID:Addgene_52963) packaged as described above by co-transfection into 293FT cells. The stable cells were selected with puromycin as indicated above and cultured in presence of doxycycline (2 μg/mL) for up to 3 passages to establish the stable 4T1-Wisp1KO (4T1 cells with CRISPR/Cas9 knockout of *Wisp1*) and 4T1-gCont (control gRNA) cell lines.

To generate 4T1-GFP cells, 4T1 cells were stably transduced with a GFP-expressing lentiviral vector (pCDH-EF1-MCS-T2A-copGFP vector; System Biosciences Cat# CD526A-1) as described above.

Preparation of conditioned medium from stable cell lines for solid-phase binding assays

To prepare conditioned medium from 4T1 stable cells, 10^6 cells were seeded in regular culture medium in 10-cm dishes and incubated for 48 h. The tissue culture–conditioned medium was then collected, filtered through a 0.2-μm filter (Nalgene), concentrated to a 1 mL final volume using a 3-kDa cut-off Amicon Ultra centrifugal filters (EMD Millipore) and used in binding assays and ELISA assays as described below. For the binding assay with coincubation of different conditioned media, culture was done in the presence of 5 μM TGFβR1 inhibitor, *SB*-431542 (Cayman Chemical, Cat# 13031) to limit endogenous WISP1 production. After 48 h, the tissue culture–conditioned medium was collected and filtered through a 0.2-μm filter (Nalgene). 4T1-Wisp1, 4T1-Wisp2, 4T1-Wisp1ΔCT, or 4T1-Wisp2+CT conditioned media were mixed with 4T1-EV or 4T1-Wisp1-myc conditioned media at 1:1 ratios, incubated on a rotator at room temperature for 45 min, and added to collagen-coated wells in 96-well plates. The plates were incubated for 2 h at 37ºC. After 3 washes with 1X wash buffer, HRP-conjugated anti-WISP1 antibody (from the mouse WISP1 Quantikine ELISA Kit, R and D Systems Cat# MWSP10), HRP-conjugated-anti-Myc (Thermo Fisher Scientific Cat# MA1-81357, RRID:AB_930031), or rabbit anti-mouse WISP2 (generated by Rockland Immunochemicals) followed by HRP-conjugated anti-rabbit IgG (Cell Signaling Technology Cat# 7074, RRID:AB_2099233) were added and bound proteins were detected as described in the "Solid-phase binding assay" section (see main text).

Preparation of conditioned medium from stable cell lines for Col I lattice formation

To prepare conditioned medium for Col I lattice formation, 10^6 tumor cells were seeded in 10 mL regular culture medium in six 10-cm dishes and incubated overnight. After 48 h, the tissue culture-conditioned medium was collected and filtered through a 0.2-µm filter (Nalgene). 60 mL of conditioned medium was then loaded into two 3-kDa cut-off Amicon Ultra centrifugal filters (EMD Millipore) and centrifuged at 4,000 g for 30 min. The concentrate (containing proteins with a molecular weight > 3 kDa) was then washed in 15 mL PBS/filter and centrifuged at 4,000 g for 30 min. The concentrate from the two filters was then pooled, mixed with 15 mL PBS, reloaded into a 3-kDa cutoff Amicon Ultra centrifugal filter, and centrifuged at 4,000 g for 30 min. The concentrate was then washed one last time with 15 ml PBS and centrifuged at 4,000 g for 50 min. The washed concentrate (1mg/mL final concentration) was then added in a 1:4 (v/v) ratio to the Col I stock solution and lattices prepared as described above.

ELISAs

WISP1 levels were detected in tissue culture–conditioned medium (48 h) with the Mouse WISP1 Quantikine ELISA kit or with Human or Mouse WISP1 DuoSet ELISA kits (R and D Systems). WISP1-myc was quantified by using anti-WISP1 antibody-coated plates from the Mouse WISP1 Quantikine ELISA kit (R and D Systems Cat# MWSP10) and an HRP-conjugated anti-Myc (Thermo Fisher Scientific Cat# MA1-81357, RRID:AB_930031) as detection antibody. WISP2 was detected with the DuoSet ELISA Ancillary Reagents kit (R and D Systems Cat# DY008), anti-mouse WISP2 (generated by Rockland Immunochemicals) and HRP-conjugated anti-rabbit IgG (Cell Signaling Technology Cat# 7074, RRID:AB_2099233).

Time-lapse migration assay

Time-lapse migration assays were performed essentially as described previously (1). Tumor cells were co-transfected with pCIG2-LifeAct-GFP (to express a cytoplasmic marker) and pCIG2-mCherryH2B (to express a nuclear marker) with Lipofectamine 3000 (Invitrogen) according to the manufacturer's protocol. Col I solutions were neutralized on ice and supplemented with WISP1 and WISP2 proteins as described in the Scanning Electron Microscopy section above. 100 µL of neutralized Col I solution was then layered onto an 8-well µ-Slide (ibidi) and incubated at 37ºC for 3 h. Col I lattices were then washed three times with RPMI. 24 h post-transfection, the cells were treated with trypsin, resuspended in RPMI 10% FCS, 1% penicillin/streptomycin and plated onto Col I lattices or uncoated wells (plastic). Cells were incubated for 4 h at 37 ºC before imaging on a 3i Marianas system configured with a Yokagowa CSU-X spinning disk confocal microscope. For some experiments, the cells were plated in RPMI or RPMI plus 2 ng/mL of recombinant TGFβ1 (R and D Systems, Cat# 240-B) 24 h before imaging. A 20x Zeiss objective, and the 488 (GFP), and 561 (RFP) laser lines were used for imaging, as described previously (1). Briefly, 30-µm Z-stacks at multiple x, y stage positions were obtained for a 12-h period at 10-minute intervals. From each 4D movie collected by using the SlideBook software (3i, RRID:SCR_014300), cells were only included in the analysis if they expressed the appropriate fluorophores and could be observed in 13 consecutive frames (2-h time frame). Cells meeting these criteria were manually tracked from each movie, and the parameters of interest were logged and exported for analysis. DiPer, an open-source computer program, was used to compute and plot the cell trajectories arising from the origin and the average cell speed. Some tracks in the Col I and Col I + WISP1 groups in Fig. 2D and in the 4T1-EV and 4T1-WISP1 groups in Supplementary Fig. S3I were previously shown (1).

Invasion and migration assays

Collagen solutions were prepared as described in the Scanning Electron Microscopy section. Collagen solutions (12.5 µL) were then layered onto membranes of 96-well Fluoroblok Transwell inserts with 8-µm pore size (Corning) and incubated at 37ºC for 3h. Col I lattices were then washed three times with RPMI or DMEM and 7,500 CellTracker Green–stained tumor cells were seeded into the insert. For some experiments, recombinant WISP1 (500 ng/mL), recombinant WISP2 (1 µg/mL, 332 ng/mL or 166 ng/mL for 1:3, 1:1 and 1:0.5 WISP1:WISP2 molar ratios, respectively), or recombinant TGFβ1 (2 ng/mL) were added to tumor cells at the time of cell seeding. RPMI + 5% FBS (for 4T1 cells) or DMEM + 5% FBS (for MDA-MB-231 cells) was used as a chemoattractant in the lower chamber. After 24 h, cells that invaded to the bottom chamber were imaged with an Olympus IX70 fluorescence inverted microscope (4 x objective) and the DP Manager software (ver. 3.3.1.222; Olympus). Invaded cells in each image were counted with the NIH ImageJ software or CellProfiler software (5, 6). Migration assays were performed as above, with non-coated Fluoroblok Transwell inserts. Some data points in the Col I and Col I + WISP1 groups in Fig. 2H and K, and in the 4T1-EV and 4T1-WISP1 groups in Fig. 3G were previously shown (1).

Proliferation assay

The number of viable cells was determined with the CellTiter-Glo luminescent ATP assay (Promega). For proliferation on collagen lattices, collagen solutions were neutralized on ice and supplemented with recombinant WISP1 and WISP2 as described for Scanning Electron Microscopy. They were then layered in 96-well plates and incubated at 37ºC for 4h (Col I) or at

room temperature for 2 h (telo-Col I). Collagen lattices were then washed three times with RPMI or DMEM, and tumor cells in RPMI + 10% FBS (for 4T1 cells) or DMEM + 10% FBS (for MDA-MB-231 cells) were added at a density of 3,000 cells per 150 µL of culture medium per well. After 24, 48, 72 h, and 96 h the culture medium was removed and 50 µL PBS + 50 µL CellTiter-Glo luminescent viability assay lysis reagent was added in each well. The plate was incubated at room temperature for 12 min on a rotating platform. 80 µL of cell lysate were then transferred to a white 96-well plate, and luminescence was detected with an Infinite M200Pro plate reader and the i-control 1.10 software (Tecan). Some data points in the Col I and Col I + WISP1 groups in Fig. 2M, and in the control and WISP1 groups in Supplementary Fig. S2N were previously shown (1).

RNA-seq and data analysis

RNA was isolated from total cell lysates with the RNeasy Plus Mini kit (Qiagen), prepared for RNA-seq with the TruSeq stranded mRNA library preparation kit (Illumina) and sequenced on the Illumina HiSeq 2000 platform. Sequences derived from total RNA paired-end 100-bp sequences were mapped to the mouse mm9 genome with the STRONGARM pipeline, which uses BWA (RRID:SCR_010910) and STAR aligner (RRID:SCR_015899) (7). Transcript-level data were counted with HTSeq (RRID:SCR_005514), and raw counts were voom-normalized and contrasted to determine differentially expressed genes by using the empirical Bayes method in limma in R 3.2.3 (RRID:SCR_010943) (8).

RT-qPCR analysis

RNA was isolated from total cell lysates with the RNeasy Mini kit (Qiagen), and reverse transcribed with the iScript™ cDNA Synthesis kit (Bio-Rad). RT-qPCR was performed with the iQ SYBR Green Supermix (Bio-Rad). Primers used were *Wisp1*(vWC domain) forw 5′-TAG GAG TGT GTG CAC AGG TGG-3′, *Wisp1*(vWC domain) rev 5′-CGT GCC ATC AAT GCA GGT ACA-3′, *Wisp1*(CT domain) forw 5′-AAG TCC AAG ACC ATC AGT GTG-3′, *Wisp1*(CT domain) rev 5′-AGG GTA AGA TTC CAA GTC AGC-3′, *Wisp2* forw 5′-CCA CGC CCC AGG AGA ATA CA-3′, *Wisp2* rev 5′-GGG CAG AAA GTT GGT GTC CTT G-3′*, Acta2* forw 5′- GCT GGT GAT GAT GCT CCC A-3′, *Acta2* rev 5′- GCC CAT TCC AAC CAT TAC TCC-3′, *18s rRNA* forw 5′-AGA AAC GGC TAC CAC ATC CAA-3′, *18s rRNA* rev 5′-GGG TCG GGA GTG GGT AAT TT-3′, *WISP1* forw 5′-GTA TGT GAG GAC GAC GCC AAG-3′, WISP1 rev 5′-GGC TAT GCA GTT CCT GTG CC-3′, *WISP2* forw 5′-TGA GAG GCA CAC CGA AGA CC-3′, *WISP2* rev 5′-GCT GGG TAC GCA CCT TTG A-3′, *GAPDH* forw 5′-CGT GGA AGG ACT CAT GAC CA-3′, *GAPDH* rev 5′-GCC ATC ACG CCA CAG TTT C-3′. Data were normalized to *18s rRNA* or *GADPH* expression. Relative mRNA levels were calculated with the comparative CT method with the CFX Manager software version 3.1 (Bio-Rad, RRID:SCR_017251).

Immunoblotting

Immunoblot analysis was performed as described previously (9). The primary antibodies were anti-mouse WISP1 (R and D Systems Cat# AF1680, RRID:AB_2216615), anti-mouse WISP1 raised against the CT domain (Boster Cat# PA2089), anti-human WISP1 (R and D Systems Cat# AF1627, RRID:AB_2216596), anti-mouse WISP2 (generated by Rockland Immunochemicals),

anti-human WISP2 (Thermo Fisher Scientific Cat# PA5-77219, RRID:AB_2720946), anti-MycTag (Cell Signaling Technology Cat# 2276, RRID:AB_331783), and anti-α-tubulin (Cell Signaling Technology Cat# 2125, RRID:AB_2619646). The secondary antibodies were horseradish peroxidase–conjugated anti-sheep (Jackson ImmunoResearch Labs Cat# 713-035-003, RRID:AB_2340709), anti-goat (Jackson ImmunoResearch Labs Cat# 705-005-147, RRID:AB_2340385), anti-rabbit (Cell Signaling Technology Cat# 7074, RRID:AB_2099233) or anti-mouse (Cell Signaling Technology Cat# 7076, RRID:AB_330924) IgG.

Mouse models of breast cancer progression and metastasis

For primary tumor growth and spontaneous metastasis, 8 to 12-week-old syngeneic wild-type BALB/c (Taconic Cat# BALB) or NSG (The Jackson Laboratory Cat# 005557) female mice were randomized and anesthetized with isoflurane, and 10^6 tumor cells resuspended in 200 μL HBSS were injected into the 4th mammary fat pad. Mice were euthanized 28 days (4T1) or 70 days (MDA-MB-231) later with CO_2 and the primary tumors were resected, weighed, and cut in 2 pieces. One piece was embedded in OCT on dry ice, and the other piece was fixed in 4% formaldehyde for 24 h. Lungs were fixed by tracheal perfusion with HBSS with 4% formaldehyde for 15 min and removed en bloc. The lung lobes were then embedded in OCT or fixed in 4% formaldehyde for 24 h. Lung sections were then prepared, stained with haematoxylin and eosin (H&E) and imaged. The number of metastases per animal was determined by counting metastatic foci in 2 H&E-stained lung sections per mouse. The metastasis count was then divided by the area covered by the lung sections to yield the number of metastases per mm^2 of lung tissue. All mice were housed and handled in accordance with approved St. Jude Children's Research Hospital Institutional Animal Care and Use Committee protocols.

Picrosirius red staining and polarized light microscopy

OCT-embedded frozen sections (10-µm-thick) were stained with a picrosirius red stain kit (Polyscience) according to the manufacturer's instructions. Briefly, sections were fixed in 4% formaldehyde for 10 min, stained in picrosirius red solution for 90 min, rinsed in 0.1 N HCl (2 × 1 min), and dehydrated in 70% ethanol for 30 sec. The slides were then dried and mounted in Permount (Fisher Chemical). The sections were imaged under polarized light or conventional light with an Olympus BX60 microscope and the cellSens Standard 1.8.1 software (Olympus, RRID:SCR_014551). The microscope settings (light intensity, condenser opening, exposure time, and gain) were kept constant throughout the imaging of all samples. Five images per tumor were taken and quantified with the CellProfiler software (RRID:SCR_007358), using constant thresholding conditions enabling exclusion of background residual light and detection and quantitation of fibrillar collagen. The average picrosirius red staining intensity for each tumor is reported. The diameters (width) and length of collagen fibers were measured with a similar approach as for SEM images, using the Autocontex machine-learning method implemented in the open-source ilastik software package to segment images (2, 3) and the FibrilJ plugin in ImageJ (4). The average diameter of the 10 longest collagen fibers in each image is reported.

Confocal and second harmonic generation (SHG) microscopy

SHG imaging of 10-µm-thick OCT-embedded frozen sections was performed with a Zeiss LSM 780 microscope with a 20x objective. Second harmonic signal was generated by illumination at 840 nm (Coherent Chameleon Ti:sapphire femtosecond laser) and detection of signal between

395 and 442 nm at a single-channel PMT. Images were acquired with the ZEN Digital Imaging for Light Microscopy software (Zeiss, RRID:SCR_013672).

Atomic force microscopy (AFM)

Samples were prepared and analyzed as previously described (1), with minor modifications. 30-µm-thick frozen sections of OCT-embedded tumors were cut on poly-L-lysine-coated slides. Sections were thawed at room temperature for 30 min. OCT was then rinsed with PBS for 15 min and slides were immediately frozen until AFM experiments. AFM measurements were taken in PBS. Data were collected using a Bruker BioScope II Controller (Bruker Corporation) integrated with a Nikon TE2000-E inverted optical microscope. Force curves from at least 20 randomly chosen points per tumor section were registered using Novascan colloidal AFM probes consisting of a 5-µm-diameter borosilicate glass particle attached to the edge of a silicon nitride V-shaped cantilever with a nominal spring constant of 0.24 N/m. The cantilever was calibrated for its laser sensitivity using the thermal oscillation method prior to each experiment. Indentation curves were captured using 4-µm ramp sizes, corresponding to an indentation depth of ~40 nm, a scan rate of 0.5 Hz, and a trigger threshold with a maximum load of 10 nN. Young's modulus was calculated following the Hertz model (spherical indenter radius = 2.5 µm) with a Poisson's ratio of 0.5, using the NanoScope Analysis software version 1.5 (Copyright Bruker Corporation).

Immunofluorescence staining

Immunofluorescence staining was performed on 10-µm-thick OCT-embedded frozen sections. Sections were fixed in acetone and stained with anti-type I collagen (Abcam Cat# ab34710, RRID:AB_731684). The secondary antibody was Alexa 568-conjugated donkey anti-rabbit IgG

(Thermo Fisher Scientific Cat# A10042, RRID:AB_2534017). Sections were mounted using Vectashield antifade mounting medium (Vector Laboratories) and imaged with a Zeiss Axio Imager 2 microscope and the ZEN software (Zeiss). Type I collagen staining intensity was quantified in 5 images per tumor with the CellProfiler software. The average type I collagen staining intensity for each tumor is reported.

Isolation of CAF-enriched stromal cells and 4T1-GFP cells from tumors

4T1-GFP tumor cells (1-4x10^6 in 200-300 µL PBS) were injected into the 4th mammary fat pads of BALB/c females. Mice were euthanized with CO_2 2-3 weeks after injection and the primary tumors were resected. These tumors were minced with razor blades and then digested with 20 mg/mL collagenase/dispase (Sigma Cat# 11 097 113 001) and 125 U/mL DNase I (Sigma Cat# 045 362 820 01) in serum-free RPMI for 2 h, removing cells and refreshing media after 1 h. The resulting cell suspension was strained first through a 70-µm mesh strainer to remove debris, then through a 40-µm mesh strainer to obtain a single cell suspension. Cells were then washed 3 X with 50 mL PBS/10 mM HEPES/0.5% FBS/5 mM EDTA, and stained with fluorophore-conjugated antibodies [anti-mouse CD45-PE (BioLegend Cat# 103106, RRID:AB_312971), CD31-APC (BioLegend Cat# 102410, RRID:AB_312905), and Gr-1-PE/Cy7 (BioLegend 108416, RRID:AB_313381)] as well as DAPI. FACS analysis was performed on a BD FACSAria Fusion Cell Sorter using BD FACSDiva 8.0.1 software (RRID:SCR_001456). Fluorescence minus one (FMO) controls were used to set the gates for CD31-APC, CD45-PE, and Gr-1-PE/Cy7. Viability and singlets gates were used to isolate single live cells, and cells which were $CD45^+$, $CD31^+$, or $Gr\text{-}1^+$ were removed. The $CD45^-$ $CD31^-$ $Gr\text{-}1^-$ cells were then sorted into GFP^+ (4T1-GFP) and GFP^- (tumor stroma, enriched for cancer-associated fibroblasts

(CAFs)). The cells were then pelleted by centrifugation and RNA extraction performed with the Quick-RNA MicroPrep Kit (ZymoReseach Cat# R1050). For some experiments, cell suspensions were plated in 10-cm tissue culture dishes and expanded in RPMI, 10% FCS, 1% penicillin/streptomycin, FACS sorted based on GFP expression, and treated with 2 ng/mL of recombinant TGFβ1 (R and D Systems, Cat# 240-B) for 24 h before RNA extraction.

SUPPLEMENTARY FIGURES AND LEGENDS

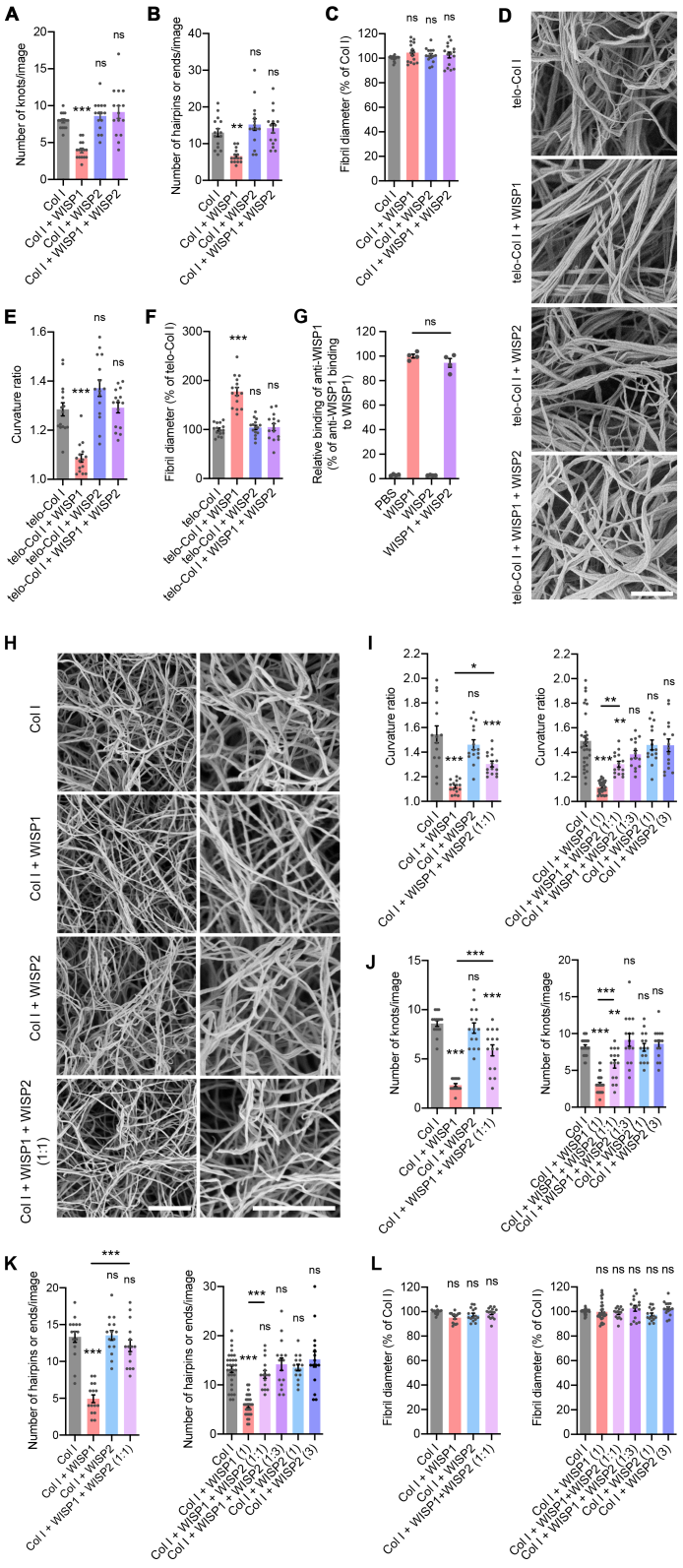

Supplementary Figure S1

Supplementary Figure S1. WISP2 inhibits WISP1-induced Col I linearization.

A and **B,** Quantitation of "knot-like" (**A**) and "hairpin- or end-like" (**B**) structures in scanning electron microscopy images of Col I lattices from Fig. 1A (n=15, 3 independent experiments, 5 images/lattice).

C, Relative fibril width (diameter) in scanning electron microscopy images of Col I lattices from Fig. 1A (n = 15, 3 independent experiments, 5 images/lattice).

D, Scanning electron microscopy of telo-Col I lattices formed in the presence of PBS, 50 µg/mL recombinant WISP1, 100 µg/mL recombinant WISP2 and 50 µg/mL WISP1 + 100 µg/mL WISP2 (1:3 WISP1:WISP2 molar ratio). Scale bar, 2 µm.

E, Curvature ratios of telo-Col I fibrils in lattices from **D** (n=15, 3 independent experiments, 5 images/lattice).

F, Relative fibril width (diameter) in scanning electron microscopy images of Col I lattices from **D** (n = 15, 3 independent experiments, 5 images/lattice).

G, ELISA for WISP1 (using the same detection antibody as for the solid-phase binding assay in Fig. 1E) in the presence of 1000:1 WISP2:WISP1 molar ratio. This data indicates that WISP2 does not interfere with the detection of WISP1 by the anti-WISP1 antibody (n=4, from 2 independent experiments).

H, Scanning electron microscopy of Col I lattices formed in the presence of PBS, 50 µg/mL recombinant WISP1, 31 µg/mL recombinant WISP2 and 50 µg/mL WISP1 + 31 µg/mL WISP2 (1:1 WISP1:WISP2 molar ratio). Scale bar, 2 µm.

I, Curvature ratios of Col I fibrils in lattices from **H** (n=15, 3 independent experiments, 5 images/lattice). Graph on the right combines data from Fig. 1B (1:3 molar ratio) and graph on the left (1:1 molar ratio).

J and **K,** Quantitation of "knot-like" (**J**) and "hairpin- or end-like" (**K**) structures in scanning electron microscopy images of Col I lattices from **H** (n=15, 3 independent experiments, 5 images/lattice). Graphs on the right combines data from Supplementary Fig. S1A and B (1:3 molar ratio) and graphs on the left (1:1 molar ratio).

L, Relative fibril width (diameter) in scanning electron microscopy images of Col I lattices from **H** (n = 15, 3 independent experiments, 5 images/lattice). Graph on the right combines data from Supplementary Fig. S1C (1:3 molar ratio) and graph on the left (1:1 molar ratio).

(A-C, E-G, I-L) mean ± SEM, one-way ANOVA followed by Tukey's posttest. ns, $P>0.05$; *, $P<0.05$; **, $P<0.01$; ***, $P<0.001$.

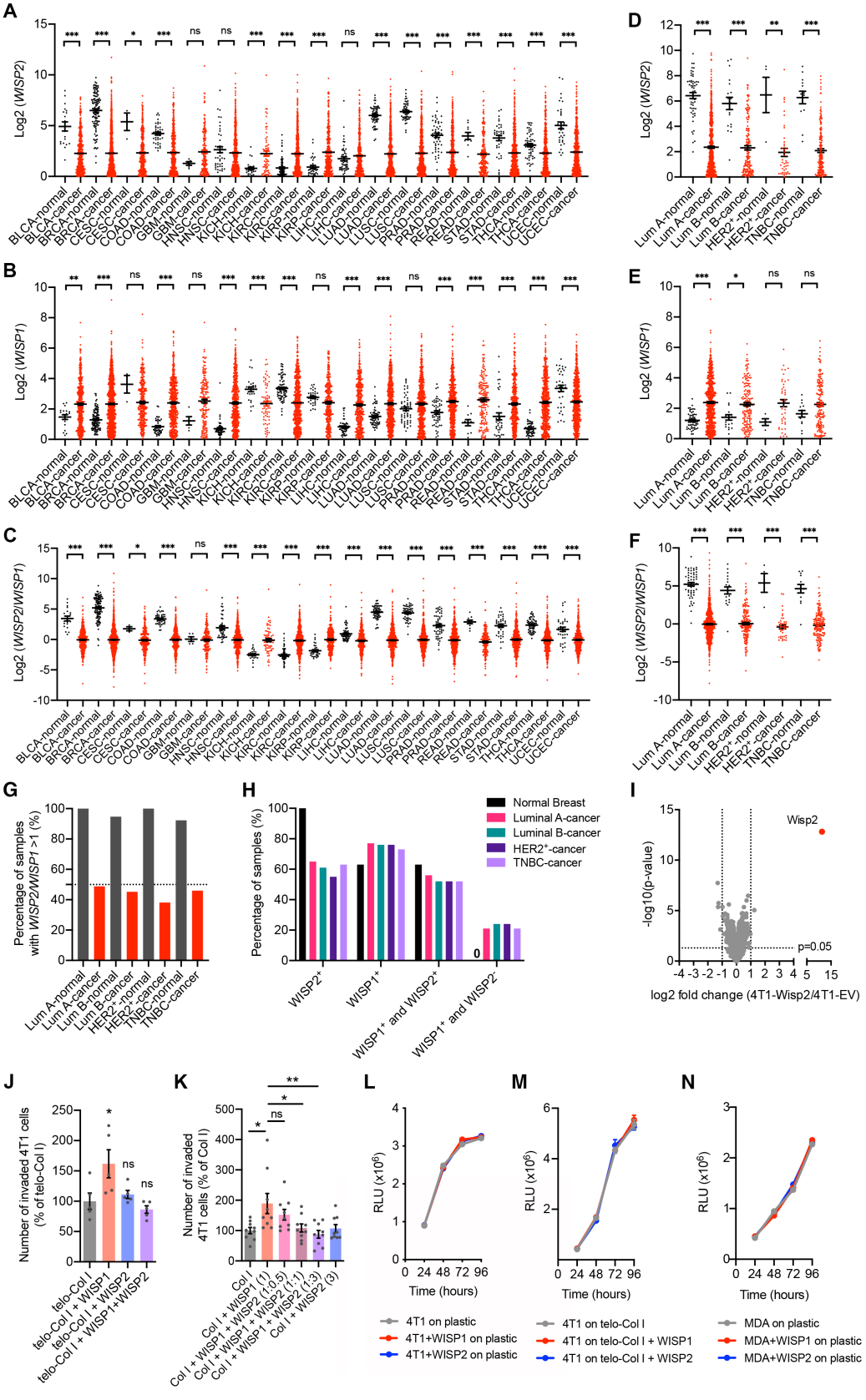

Supplementary Figure S2

Supplementary Figure S2. WISP2 is less abundant in tumors than in adjacent normal tissues and is an inhibitor of WISP1-induced tumor cell invasion though Col I.

A-C, *WISP2* (**A**) or *WISP1* (**B**) gene expression levels, or *WISP2/WISP1* gene expression ratio (**C**) in tumors and adjacent normal tissues from patients with different cancer types (BLCA, bladder urothelial carcinoma, n=19 normal and n=414 tumors; BRCA, breast invasive carcinoma, n=113 normal and n=1119 tumors; CESC, cervical squamous cell carcinoma and endocervical carcinoma, n=3 normal and n=306 tumors; COAD, colon adenocarcinoma, n=41 normal and n=483 tumors; GBM, glioblastoma multiforme, n=5 normal and n=170 tumors; HNSC, head and neck squamous cell carcinoma, n=44 normal and n=504 tumors; KICH, kidney chromophobe, n=25 normal and n=66 tumors; KIRC, kidney renal clear cell carcinoma, n=72 normal and n=542 tumors; KIRP, kidney renal papillary cell carcinoma, n=32 normal and n=291 tumors; LIHC, liver hepatocellular carcinoma, n=50 normal and n=374 tumors; LUAD, lung adenocarcinoma, n=59 normal and n=541 tumors; LUSC, lung squamous cell carcinoma, n=51 normal and n=502 tumors; PRAD, prostate adenocarcinoma, n=52 normal and n=502 tumors; READ, rectum adenocarcinoma, n=10 normal and n=167 tumors; STAD, stomach adenocarcinoma, n=37 normal and n=420 tumors; THCA, thyroid carcinoma, n=59 normal and n=513 tumors; UCEC, uterine corpus endometrial carcinoma, n=35 normal and n=554 tumors).

D-F, *WISP2* (**D**) or *WISP1* (**E**) gene expression levels, or *WISP2/WISP1* gene expression ratio (**F**) in tumors and adjacent normal tissues from patients with different subtypes of breast cancer (Lum A, Luminal A breast cancer, n=55 normal and n=614 tumors; Lum B, Luminal B breast cancer, n=19 normal and n=157 tumors; HER2+, HER2-enriched breast cancer, n=4 normal and n=42 tumors; TNBC, triple-negative breast cancer, n=13 normal and n=161 tumors).

G, Percentage of samples from breast cancer patients with a *WISP2/WISP1* ratio>1.

H, Percentage of samples from breast cancer patients with *WISP1* or *WISP2* gene expression levels >1 TPM.

I, Volcano plots of transcripts detected by RNA-seq. The x-axis shows Log2 ratios of gene expression comparing 4T1-Wisp2 with 4T1-EV cells (n=3 biological replicates).

J, Invasion of 4T1 cells through telo-Col I, telo-Col I + WISP1, telo-Col I + WISP2 or telo-Col I + WISP1 + WISP2 lattices layered on Transwell inserts (n=5 biological replicates).

K, Invasion of 4T1 cells through Col I layered on Transwell inserts, in the presence of different molar ratios (1:0.5, 1:1, and 1:3) of WISP1 and WISP2 (n=9, from 3 independent experiments).

L, Proliferation rate of 4T1 cells plated on plastic in the presence of vehicle, or 500 ng/mL WISP1 or WISP2 (n=4 biological replicates).

M, Proliferation rate of 4T1 cells plated on telo-Col I, telo-Col I + WISP1 or telo-Col I + WISP2 (n=4 biological replicates).

N, Proliferation rate of MDA-MB-231 cells plated on plastic in the presence of vehicle, 500 ng/mL WISP1 or WISP2 (n=4 biological replicates).

(A-F, J-M) Mean ± SEM, (A-F) Mann-Whitney test, (J, K) one-way ANOVA followed by Tukey's posttest. ns, $P>0.05$; *, $P<0.05$; **, $P<0.01$; ***, $P<0.001$.

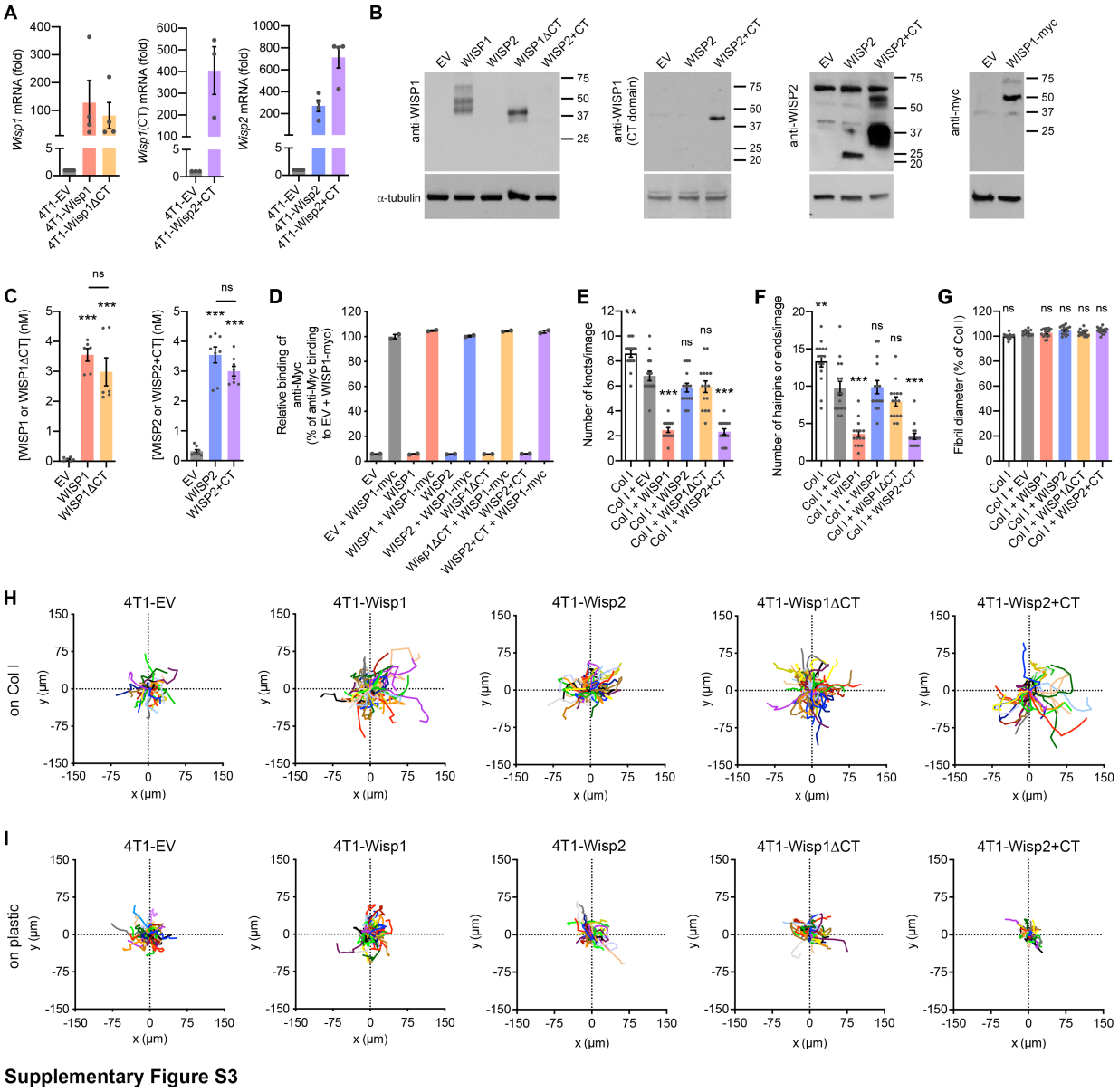

Supplementary Figure S3

Supplementary Figure S3. The C-terminal domain of WISP1 drives WISP1-induced cell invasion through Col I but is dispensable for WISP1-Col I binding.

A, Relative expression levels of *Wisp1* and *Wisp2* constructs in the 4T1-EV, 4T1-Wisp1, 4T1-Wisp1ΔCT, 4T1-Wisp2, and 4T1-Wisp2+CT cell lines. Left panel, primers amplifying a sequence coding for the VWC domain of *Wisp1* were used. Middle panel, primers amplifying a

sequence coding for the CT domain of *Wisp1* were used. Right panel, primers for *Wisp2* were used (n=3 independent experiments).

B, Expression levels of WISP constructs in 4T1-EV, 4T1-Wisp1, 4T1-Wisp2, 4T1-Wisp1ΔCT, 4T1-Wisp2+CT, and 4T1-Wisp1-myc cell lines, detected by Western blot using anti-WISP1 (1st panel), anti-WISP1 raised against the CT domain of WISP1 (2nd panel), anti-WISP2 (3rd panel; WISP2 band ~25 kDa; WISP2+CT band;~37 kDa) or anti-Myc (4th panel). α-tubulin was used as loading control.

C, Expression levels of WISP constructs in conditioned medium from the 4T1-EV, 4T1-Wisp1, 4T1-Wisp1ΔCT, 4T1-Wisp2, and 4T1-Wisp2+CT cell lines, detected by ELISA using anti-WISP1 (left) or anti-WISP2 (right) (n= 6-8, from 3-4 independent experiments).

D, ELISA for WISP1-myc (using the same detection anti-Myc antibody as for the solid-phase binding assay in Fig. 3C) in the presence of conditioned medium from 4T1 cells overexpressing WISP1, WISP1ΔCT, WISP2 or WISP2+CT. These data indicate that these conditioned media do not interfere with the detection of WISP1-myc by the anti-Myc antibody (n=2 replicates).

E and **F,** Quantitation of "knot-like" (**E**) and "hairpin- or end-like" (**F**) structures in scanning electron microscopy images of Col I lattices from Fig. 3D (n=15, 3 independent experiments, 5 images/lattice).

G, Relative fibril width (diameter) in scanning electron microscopy images of Col I lattices from Fig. 3D (n = 15, 3 independent experiments, 5 images/lattice).

H, Migratory tracks of 4T1-EV (n=123), 4T1-Wisp1 (n=75), 4T1-Wisp2 (n=69), 4T1-Wisp1ΔCT (n=106), and 4T1-Wisp2+CT (n=66) cells plated on Col I lattices.

I, Migratory tracks of 4T1-EV (n=115), 4T1-Wisp1 (n=89), 4T1-Wisp2 (n=54), 4T1-Wisp1ΔCT (n=53), and 4T1-Wisp2+CT (n=59) cells plated on plastic.

(A, C-G) Mean ± SEM. (C, E-G) one-way ANOVA followed by Tukey's posttest. ns, $P>0.05$; **, $P<0.01$; ***, $P<0.001$.

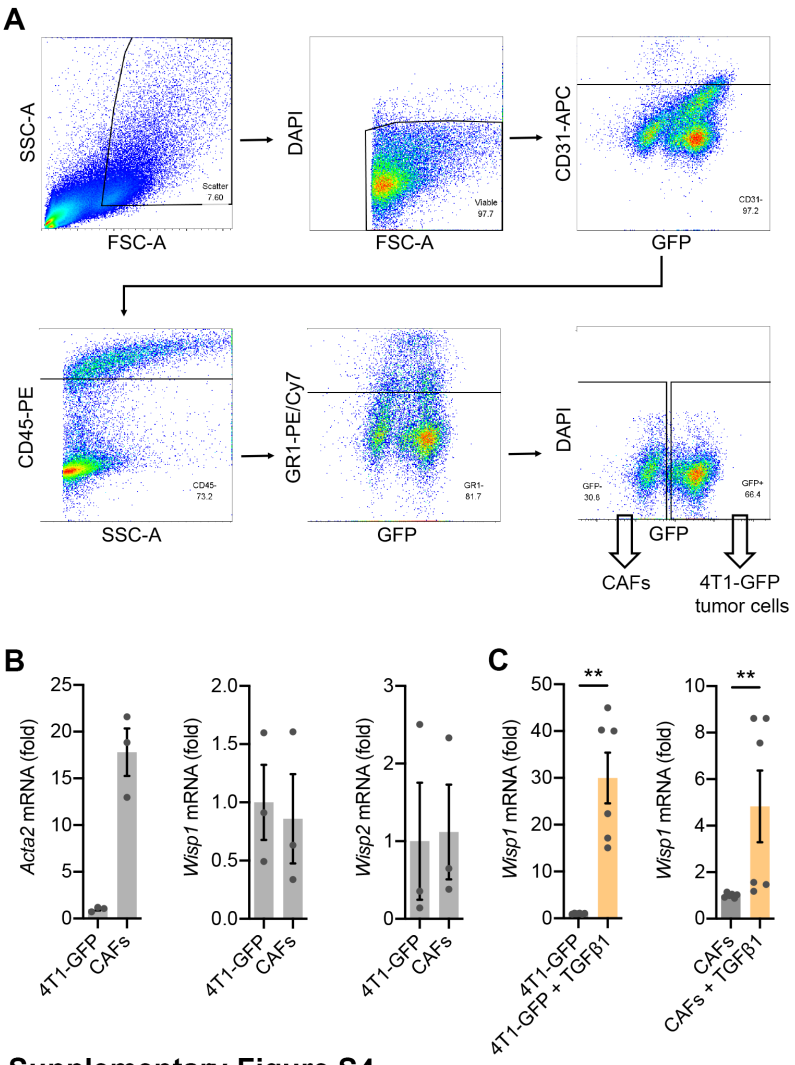

Supplementary Figure S4

Supplementary Figure S4. *Wisp1* is expressed by tumor cells and cancer-associated fibroblast (CAF)-enriched stromal cells isolated from primary breast tumors.

A, Gating strategy for sorting 4T1-GFP tumor cells and CAF-enriched stromal cells (CAFs). Successive gates remove debris, dead cells, $CD31^+$ cells, $CD45^+$ cells, $Gr\text{-}1^+$ cells, and then separate the GFP^+ (4T1-GFP tumor cells) and GFP^- (CAF-enriched stromal cells (CAFs)) populations for sorting.

B, Relative expression levels of *Acta2* (α-smooth muscle actin, a marker for CAFs; left panel), *Wisp1* (middle panel) and *Wisp2* (right panel) in 4T1-GFP and CAF-enriched stromal cells

(CAFs) isolated from primary breast tumors (n=3 tumors). The ~15- to 20-fold increase in *Acta2* mRNA levels in the GFP^- (CAFs) vs 4T1-GFP tumor cells confirms that the GFP^- stromal cell population is enriched with CAFs.

C, Relative expression levels of *Wisp1* in 4T1-GFP (left panel) and CAF-enriched stromal cells (CAFs; right panel) treated with TGFβ1 (2 ng/mL) or vehicle control (n=6, from 2 independent experiments).

(B, C) Mean ± SEM. (C, left) unpaired two-sided t-test, (C, right) Mann-Whitney test. **, $P<0.01$.

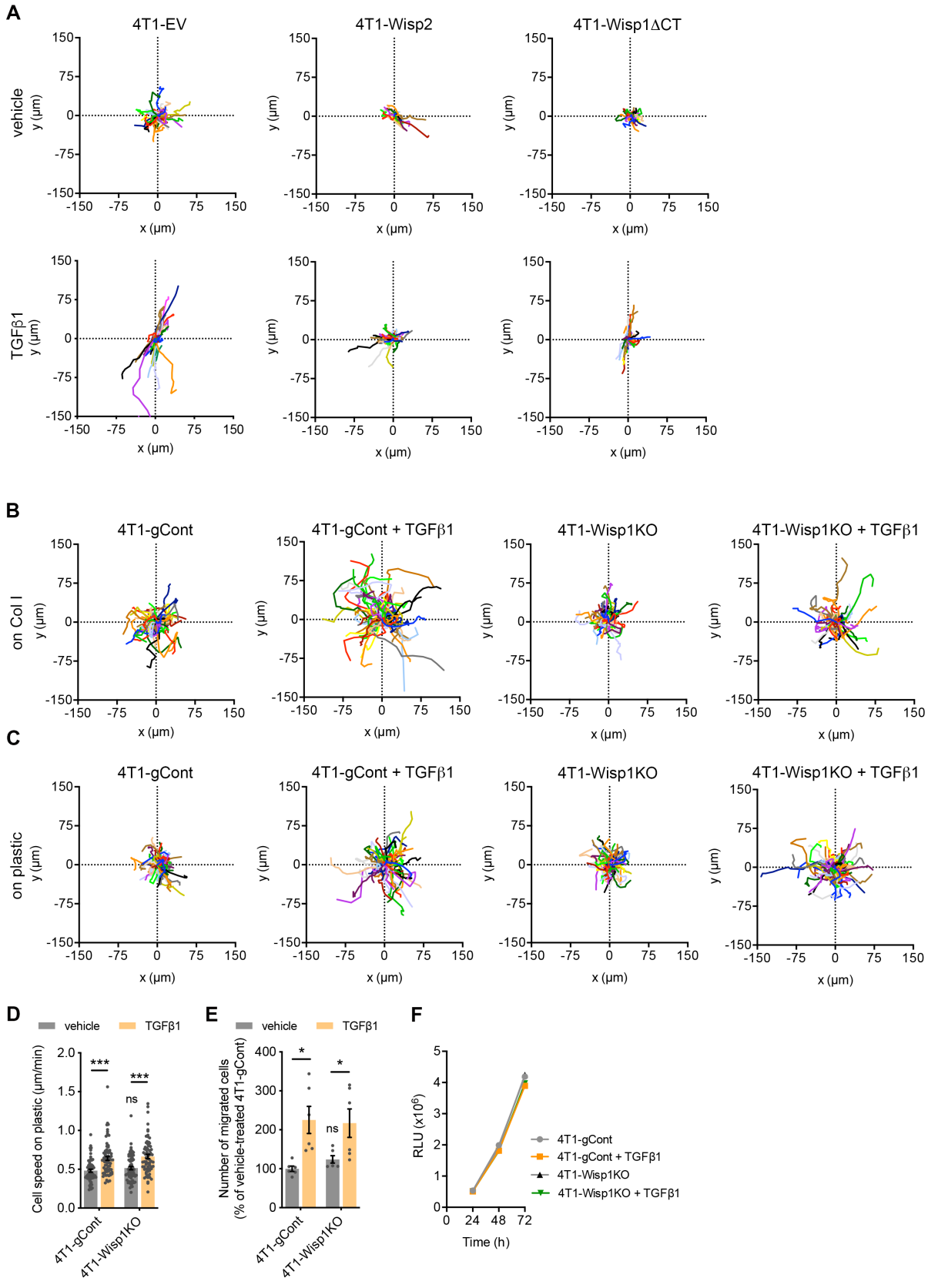

Supplementary Figure S5

Supplementary Figure S5. WISP2 and WISP1ΔCT block TGFβ1-induced cell invasion through Col I by acting as WISP1 antagonists.

A, Migratory tracks of 4T1-EV + vehicle (n=44), 4T1-EV + TGFβ1 (n=37), 4T1-Wisp2 + vehicle (n=36), 4T1-Wisp2 cells + TGFβ1 (n=44), 4T1-Wisp1ΔCT + vehicle (n=36), and 4T1-Wisp1ΔCT + TGFβ1 (n=35) cells plated on Col I lattices.

B, Migratory tracks of 4T1-gCont + vehicle (n=72), 4T1-gCont + TGFβ1 (n=64), 4T1-Wisp1KO (n=68), 4T1-Wisp1KO + TGFβ1 (n=48) cells plated on Col I lattices.

C, Migratory tracks of 4T1-gCont + vehicle (n=72), 4T1-gCont + TGFβ1 (n=64), 4T1-Wisp1KO (n=68), 4T1-Wisp1KO + TGFβ1 (n=48) cells plated on plastic.

D, Average cell speed of cells tracked in **C**.

E, Migration of 4T1-gCont and 4T1-Wisp1KO treated with TGFβ1 (2 ng/mL) or vehicle control, through uncoated Transwell inserts (n=6 biological replicates).

F, Proliferation rate for cells plated in the same conditions as in **C** (n= 8 biological replicates).

(D-F) Mean ± SEM, (D, E) two-way ANOVA followed by Tukey's posttest. ns, $P>0.05$; *, $P<0.05$; ***, $P<0.001$.

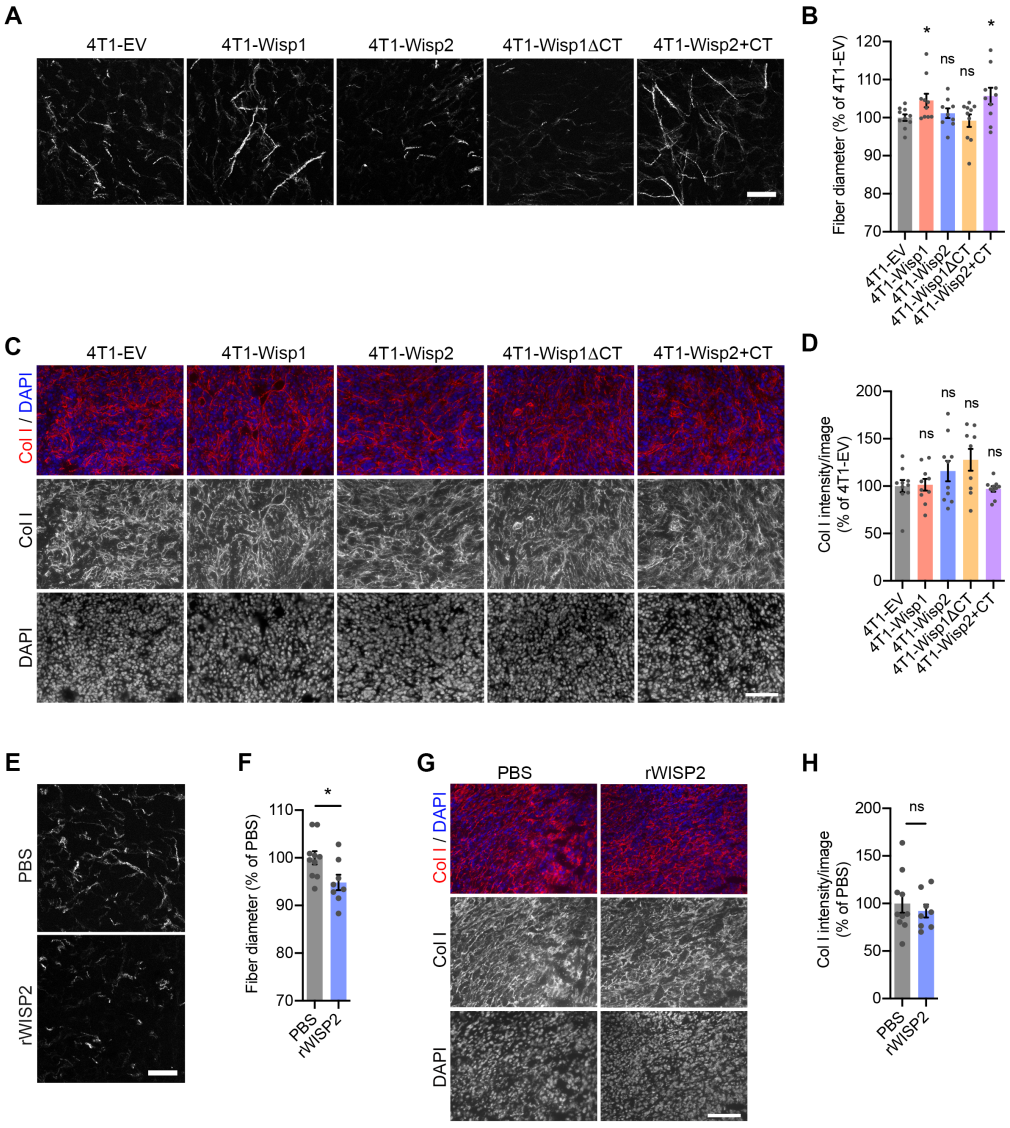

Supplementary Figure S6

Supplementary Figure S6. WISP2 limits collagen linearization but does not affect total type I collagen levels in 4T1 breast tumors.

A, Fibrillar collagen in primary tumors from Fig. 5A, visualized by second harmonic generation microscopy. Scale bar, 40 μm.

B, Average fibrillar collagen diameter in picrosirius red staining images of tumors from Fig. 5A (n=10 mice/group, except 4T1-Wisp2, n=9 mice).

C, Representative immunostaining for type I collagen in primary tumors from Fig. 5A. DAPI staining is also shown. Scale bar, 100 μm.

D, Average type I collagen staining intensity in images of tumors from Fig. 5A (n=10 mice/group, except 4T1-Wisp2, n=9 mice).

E, Fibrillar collagen in primary tumors from Fig. 5G, visualized by second harmonic generation microscopy. Scale bar, 40 μm.

F, Average fibrillar collagen diameter in picrosirius red staining images of tumors from Fig. 5G (PBS, n=10; rWISP2, n=8 mice/group).

G, Representative immunostaining for type I collagen in primary tumors from Fig. 5G. DAPI staining is also shown. Scale bar, 100 μm.

H, Average type I collagen staining intensity in images of tumors from Fig. 5G (PBS, n=10; rWISP2, n=8 mice/group).

(B, D, F, H) Mean ± SEM, (B, F, H) unpaired two-sided *t*-test, (D) one-way ANOVA followed by Tukey's posttest. ns, $P>0.05$; *, $P<0.05$.

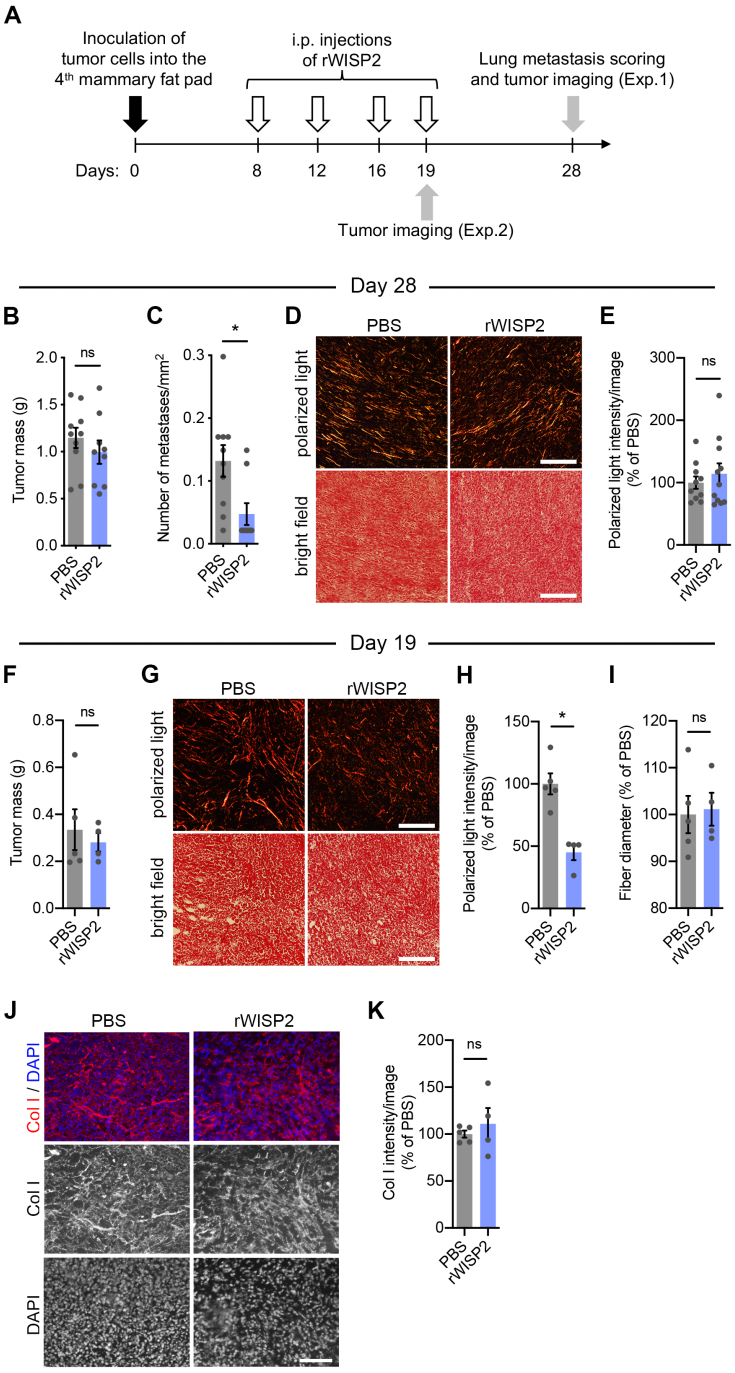

Supplementary Figure S7

Supplementary Figure S7. WISP2 limits collagen linearization in aggressive 4T1-Wisp1 tumors and inhibits breast cancer metastasis.

A, Scheme of experimental design. Recombinant WISP2 (rWISP2; 100 µg in 200 µL PBS) was administered via intraperitoneal injection on day 8, day 12, day 16, and day 19 post-injection of

4T1-Wisp1 cells. Tissues were collected on day 28 (Experiment 1) or on day 19, 2 h after the last dose of rWISP2 (Experiment 2).

B, Primary tumor mass, 28 days after orthotopic inoculation of 4T1-Wisp1 cells into the 4th mammary fat pad (PBS, n=10; rWISP2, n=9 mice/group). rWISP2 was administered via intraperitoneal injection, as illustrated in **A** (Experiment 1).

C, Numbers of lung metastases in mice from **B**.

D, Representative images of fibrillar collagen in primary tumors from **B** visualized by picrosirius red staining followed by polarized light microscopy. Corresponding bright-field images show tissue integrity. Scale bars, 200 μm.

E, Average polarized light intensity in picrosirius red staining images of tumors from **B**.

F, Primary tumor mass, 19 days after orthotopic inoculation of 4T1-Wisp1 cells into the 4th mammary fat pad (PBS, n=5; rWISP2, n=4 mice/group). rWISP2 was administered via intraperitoneal injection, as illustrated in **A** (Experiment 2). Tissues were collected 2 h after the last injection of rWISP2.

G, Representative images of fibrillar collagen in primary tumors from **F** visualized by picrosirius red staining followed by polarized light microscopy. Corresponding bright-field images show tissue integrity. Scale bars, 200 μm.

H, Average polarized light intensity in picrosirius red staining images of tumors from **F**.

I, Average fibrillar collagen diameter in picrosirius red staining images of tumors from **F**.

J, Representative immunostaining for type I collagen in primary tumors from **F**. DAPI staining is also shown. Scale bar, 100 μm.

K, Average type I collagen staining intensity in images of tumors from **F**.

(B, C, E, F, H, I, K) Mean ± SEM, (B, C, E, F, I, K) unpaired two-sided *t*-test, (H) Mann-Whitney test. ns, $P>0.05$; *, $P<0.05$.

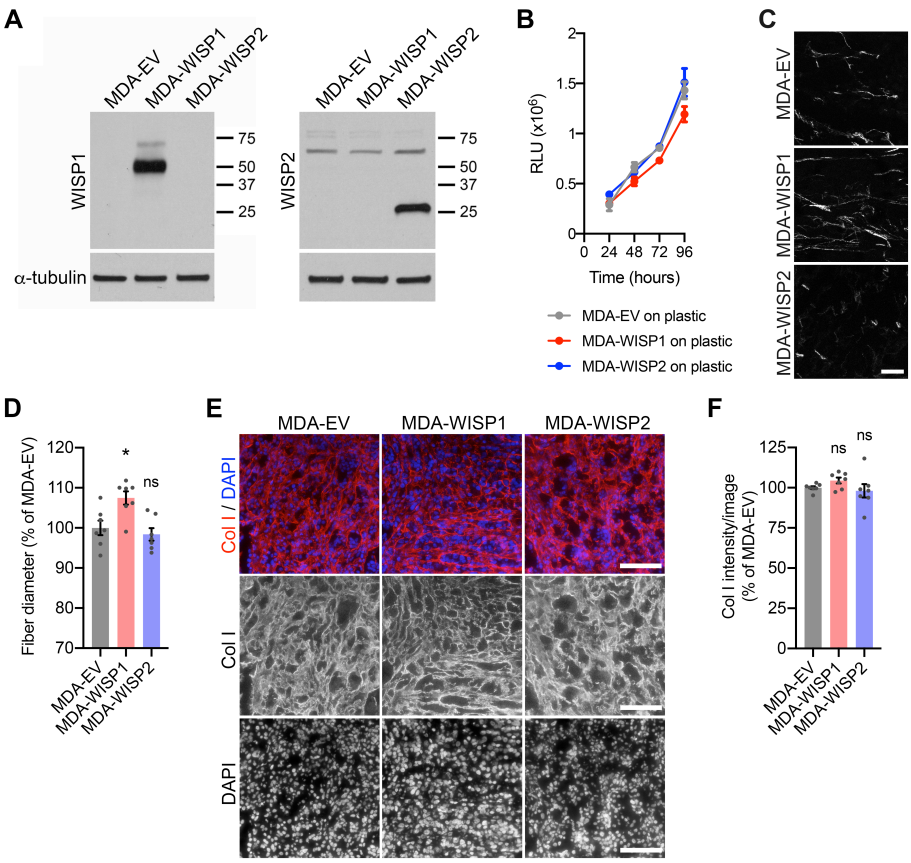

Supplementary Figure S8

Supplementary Figure S8. WISP1 promotes whereas WISP2 inhibits human breast cancer metastasis.

A, Protein expression levels of WISP1 and WISP2 in MDA-MB-231 cells stably overexpressing *WISP1* (MDA-WISP1) or *WISP2* (MDA-WISP2), or stably transduced with an empty vector control (MDA-EV), detected by Western blot. α-tubulin was used as loading control.

B, Proliferation rate of MDA-EV, MDA-WISP1, or MDA-WISP2 cells plated on plastic surface. (n= 12 biological replicates).

C, Fibrillar collagen in primary tumors from Fig. 6D, visualized by second harmonic generation microscopy. Scale bar, 40 μm.

D, Average fibrillar collagen diameter in picrosirius red staining images of tumors from Fig. 6D (n=7 mice/group).

E, Representative immunostaining for type I collagen in primary tumors from Fig. 6D. DAPI staining is also shown. Scale bar, 100 μm.

F, Average type I collagen staining intensity in images of tumors from Fig. 6D (n=7 mice/group).

(B, D, F) Mean ± SEM, (D, F) one-way ANOVA followed by Tukey's posttest. ns, $P>0.05$; *, $P<0.05$.

SUPPLEMENTARY TABLES

Supplementary Table S1. gBlock sequence for the generation of pCDH-EF1-Wisp2+CT-T2A-puro from pCDH-EF1-Wisp2-T2A-puro

gBlock name	gBlock Sequence
Wisp2-Wisp1CT	5'- caggagccacggctcatggaacagtgccttccagccagaggaggccacga acttcactctcgcaggctgtgtcagcacacgcacctaccgacccaagtac tgcggagtctgtactgacaataggtgttgcatcccctacaagtccaagac catcagtgtggatttccagtgtccagaggggccaggtttctcccggcagg tcctatggattaatgcttgcttctgcaacctgagctgcaggaatcctaac gatatctttgctgacttggaatcttaccctgacttcgaagagattgccaa tgagggcagaggaagtcttctaacatgcggtgacg-3'

Supplementary Table S2. Primers used for cloning

Primer name	Sequence	Comment
dCT-del_Wisp1_frw	5′-GCC TGG CTG TGT ACG AGG GCA GAG GAA G-3′	To generate the Wisp1ΔCT plasmid from the Wisp1 plasmid
dCT-del_Wisp1_rev	5′-CTT CCT CTG CCC TCG TAC ACA GCC AGG C-3′	To generate Wisp1ΔCT plasmid from the Wisp1 plasmid
Wisp2+CT(Wisp1)_frw	5′-CGC TGC CAC CAT GCA GCC AGA GGA GG-3′	To add the CT domain of Wisp1 to the Wisp2 plasmid
Wisp2+CT(Wisp1)_rev	5′-CCT CCT CTG GCT GCA TGG TGG CAG CG-3′	To add the CT domain of Wisp1 to the Wisp2 plasmid
Wisp1-myc_frw	5′-ACT TCG AAG AGA TTG CCA ATG AAC AAA AAC TCA TCT CAG AAG AGG ATC TGG AGG GCA GAG-3′	To add Myc tag to the Wisp1 plasmid
Wisp1-myc_rev	5′-CTC TGC CCT CCA GAT CCT CTT CTG AGA TGA GTT TTT GTT CAT TGG CAA TCT CTT CGA AGT-3′	To add Myc tag to the Wisp1 plasmid

Supplementary Table S3. gRNAs targeting *Wisp1* and of non-targeting control gRNAs

gRNA	gRNA sequence
Wisp1.g9	5′–GCCTCTACTGCGATTACAGTNGG–3′
Wisp1.g6	5′–TGCCATCTGTGACCCACACCNGG–3′
Wisp1.g43	5′–TGGTGTAGCGTACGCCATCCNGG–3′
Wisp1.g24	5′–CCAGGGACTCTCACGTGCCGNGG–3′
Wisp1.g8	5′–ACCTGCATTGATGGCACGGTNGG–3′
Negative mouse.g22 (non-targeting control)	5′–TAAGAGGGCGAAGGAGTCATNGG– 3′
Negative mouse.g24 (non-targeting control)	5′–TAGGCGAGCCTTCCAAGGATNGG–3′
Negative mouse.g27 (non-targeting control)	5′–ATGGAAGGCTCGCCTATCCTNGG–3′

SUPPLEMENTARY REFERENCES

1. Jia H, Janjanam J, Wu SC, Wang R, Pano G, Celestine M*, et al.* The tumor cell-secreted matricellular protein WISP1 drives pro-metastatic collagen linearization. *EMBO J.* **2019**;38(16):e101302.
2. Sommer C., Strähle C., Köthe U., and F.A. H. ilastik: Interactive Learning and Segmentation Toolkit. *Eighth IEEE International Symposium on Biomedical Imaging (ISBI) Proceedings.* **2011**:230-233.
3. Haubold C, Schiegg M, Kreshuk A, Berg S, Koethe U, and Hamprecht FA. Segmenting and Tracking Multiple Dividing Targets Using ilastik. *Adv Anat Embryol Cell Biol.* **2016**;219:199-229.
4. Sokolov PA, Bondarev SA, Belousov MV, Zhouravleva GA, and Kasyanenko NA. Sup35NMp morphology evaluation on Au, Si, formvar and mica surfaces using AFM, SEM and TEM. *J Struct Biol.* **2018**;201(1):5-14.
5. Carpenter AE, Jones TR, Lamprecht MR, Clarke C, Kang IH, Friman O*, et al.* CellProfiler: image analysis software for identifying and quantifying cell phenotypes. *Genome Biol.* **2006**;7(10):R100.
6. Lamprecht MR, Sabatini DM, and Carpenter AE. CellProfiler: free, versatile software for automated biological image analysis. *Biotechniques.* **2007**;42(1):71-75.
7. Dobin A, Davis CA, Schlesinger F, Drenkow J, Zaleski C, Jha S*, et al.* STAR: ultrafast universal RNA-seq aligner. *Bioinformatics.* **2013**;29(1):15-21.
8. Law CW, Chen Y, Shi W, and Smyth GK. voom: Precision weights unlock linear model analysis tools for RNA-seq read counts. *Genome Biol.* **2014**;15(2):R29.

9. Labelle M, Schnittler HJ, Aust DE, Friedrich K, Baretton G, Vestweber D*, et al.* Vascular endothelial cadherin promotes breast cancer progression via transforming growth factor beta signaling. *Cancer Res.* **2008**;68(5):1388-1397.